International Journal of Fluid Machinery and Systems
Vol. 2, No. 2, April-June 2009

Original Paper

Study on Design of Air-water Two-phase Flow Centrifugal Pump Based on Similarity Law

Naoki Matsushita, Akinori Furukawa, Satoshi Watanabe and Kusuo Okuma

Department of Mechanical Engineering, Kyushu University
744 Moto-oka, Nishi-ku, Fukuoka, 819-0395, Japan
matsushita@ryusei2.mech.kyushu-u.ac.jp, fmfuru@mech.kyushu-u.ac.jp,
fmnabe@mech.kyushu-u.ac.jp, kokuma@mech.kyushu-u.ac.jp

Abstract

A conventional centrifugal pump causes a drastic deterioration of air-water two-phase flow performances even at an air-water two-phase flow condition of inlet void fraction less than 10% in the range of relatively low water flow rate. Then we have developed a two-phase flow centrifugal pump which consists of a tandem arrangement of double rotating cascades and blades of outer cascade have higher outlet angle more than 90^{o}. In design of the two-phase flow pump for various sized and operating conditions, similarity relations of geometric dimensions to hydraulic performances is very useful. The similarity relations of rotational speed, impeller diameter and blade height are investigated for the developed impeller in the present paper. As the results, the similarity law of rotational speed and impeller diameter is clarified experimentally even in two-phase flow condition. In addition, influences of blade height on air-water two-phase flow performances indicate a little difference from the similarity relations.

Keywords: Centrifugal pump, Air-water two-phase flow, Pump performance, Similarity law

1. Introduction

Centrifugal pumps are utilized in various industrial fields due to its simple structure and easy maintenance. However, there is a strong demand to develop a gas-liquid two-phase flow centrifugal pump for diversity of transport and operation process. Especially, in the offshore oil production and aeration process of sewage disposal, a cost-reduction is desired by using a two-phase flow pump instead of using a pump and a compressor simultaneously with a gas-liquid separator[1]. Air-water two-phase flow performances of conventional centrifugal pump with the backward blades causes the severe deterioration at an inlet void fraction less than about 10% due to the strong centrifugal effect on the pump internal flow[2].

We have investigated experimentally that the development of the centrifugal pump with high air-water two-phase flow performances as a previous research. As the results, it was clarified that the suppression of air-accumulating region in the impeller is very important to improve the air-water two-phase flow performances. At the present stage, we have proposed the followings as powerful methods to avoid the impermissible deterioration of pump performance. Firstly, (1) the impeller is open for the blade tip leakage flow to suppress the air accumulating region. And, (2) a multi-bladed impeller with thin blades is effective to shear the air-accumulating region due to the rotating shear action at a blade inlet. And, (3) a higher outlet blade angle yields higher theoretical head even in two-phase flow condition. (4) A tandem arrangement of double rotating circular cascades prevents a rotating stall and the abrupt deterioration of pump head in the range of lower air-water flow rate ratio. (5) An installation of diffuser cascade downstream of the impeller outlet is powerful method to shear and suppress the elongation of air-accumulating region[3],[4],[5],[6],[7].

In general, a conventional type of centrifugal pump is designed by using similarity law of pump configuration and performances for the various design specification (flow rate Q and pump head H, etc). However, as far as we know, the similarity law of two-phase flow performances of centrifugal pump is not clarified at the present stage. In the present paper, firstly, we investigate the influences of rotational speed of impeller on air-water two-phase flow performances. Secondly, the influences of impeller diameter and blade height on air-water two-phase flow performances are discussed by comparing the experimental results of developed two-phase flow centrifugal pumps. Then we examine the similarity law of $Q \propto BD_2^{\,2}N$, $H \propto D_2^{\,2}N^2$ and $L \propto BD_2^{\,4}N^3$ in air-water two-phase flow condition in detail from the measurements of static head of pump shroud-wall.

Received April 26 2009; accepted for publication May 9 2009: Review conducted by Prof. Xi Guang. (Paper number O09011)
Corresponding author: Naoki Matsushita, Professor, matsushita@ryusei2.mech.kyushu-u.ac.jp.

2. Experimental apparatus

The sectional view of test pump with a horizontal rotating shaft is shown in Fig. 1. The smaller impeller with the diameter of D_2=190mm, called as D190 impeller, is depicted on the upside of a horizontal rotating shaft in Fig 1. And the larger impeller with the diameter of D_2=235mm, called as D235 impeller, is depicted on the downside of a horizontal rotating shaft in Fig 1. Figure 2 shows the configurations of the test impellers. Every impeller was tested in the same volute casing and the pump rotational speed was controllable by an inverter equipped against N=1250min^{-1} in design. Then, the test impeller of D190, having the vaneless diffuser downstream of impeller outlet, is diffuser pump type. On the other hand, the test impeller of D235, having no diffuser section downstream of impeller outlet, is volute pump type. Suction pressure at the position 1 in Fig. 1 is set as 0.1MPa-gage constant on the present experiment. Water in an open tank enters the test pump through a boost pump and orifice-meter for water flow rate Q_L. Compressed air is brown from a nozzle into the suction pipe through a regulator and orifice-meter for air flow rate Q_G calculated on the basis of static pressure and temperature at the suction pipe. Pump head H based on water specific weight $\rho_L \cdot$ g, where ρ_L is water density and g is the acceleration of gravity, was obtained as the difference of the measured static head and dynamic head assumed as a homogeneous flow between positions 1 and 2 in Fig. 1. Shaft power L was obtained by subtracting the mechanical torque loss in the idling of impeller in atmosphere from measured torque and multiplying the torque and the angular velocity of shaft. Flow coefficient ϕ is defined as flow rate Q divided by flow passage area A_2 and rotational speed U_2 at the

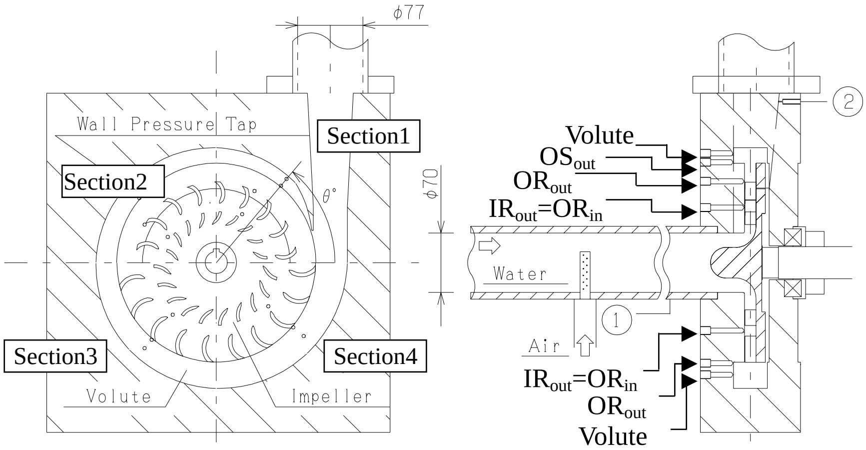

Fig. 1 The sectional view of test pump

impeller outlet, pump head coefficient ψ was normalized by U_2^2/g, and shaft power coefficient τ by $\rho_L A_2 U_2^3$. In addition to these measurements, the static pressure on shroud-wall was measured with high response pressure transducer at four radial positions, between inner and outer rotors called as $IR_{out}=OR_{in}$, 1mm downstream of impeller outlet called as OR_{out}, the outlet of diffuser section called as OS_{out} and the middle of volute passage in the radial direction called as Volute, and at four peripheral positions (Sections 1~4) as shown in Fig. 1. The measured static head is evaluated as the head difference from the static head at the position 1 of suction pipe in Fig. 1. The static head coefficient $\Delta\psi_s$ was defined as measured static head divided by U_2^2/g. Air-water behavior in the impeller was observed through the transparent casing with video camera equipment of 30fps and a stroboscopic light.

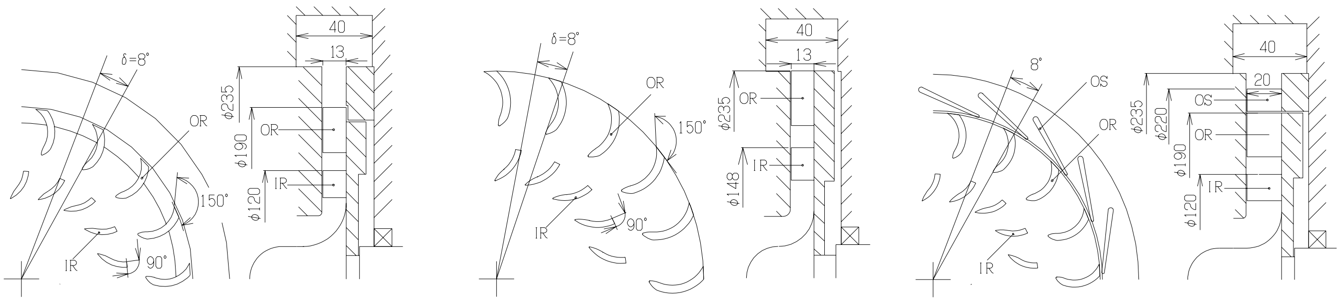

(a) D190_B13 w/o OS (b) D235_B13 (c) D190_B20 with OS

Fig. 2 Test impellers configurations

3. Results and Discussion

3.1 Similarity law of rotational speed

The similarity law of a centrifugal pump is described by $Q \propto BD_2^2N$, $H \propto D_2^2N^2$ and $L \propto BD_2^4N^3$, where D is impeller outlet diameter, B is blade height and N is rotational speed. Firstly, we investigated the similarity law of pump performances with changing the rotational speed in the 900min^{-1} to 1600min^{-1} range in the case of D190_B13 w/o OS impeller as shown in Fig. 2 (a).

D190_B13 w/o OS impeller is double rotating cascade with vaneless diffuser downstream of impeller outlet. Every impeller is designed at ϕ_L=0.08 as a shock-less entry at the impeller inlet, and the specific speed is 149(min^{-1}, m^3/min, m) in the case of D190_B13 w/o OS impeller. Figures 3 and 4 show the characteristic curves in water single-phase flow and the air-water two-phase flow at ϕ_L=0.08 constant. In addition to the performances of D190_B13 w/o OS impeller, the experimental results of SIo6 w/o OS impeller[3], as a conventional type of centrifugal impeller having single cascade and backward blades with the outlet blade angle 25° (the figure of impeller is omitted, the specific speed is 271(min^{-1}, m^3/min, m)), are shown. In the case of water single-phase flow, it is confirmed that the head coefficient ψ and shaft power coefficient τ of each impeller agree fairly well in the range of rotational speed 900~1600min^{-1} in water single-phase flow. This result indicates that the similarity law of rotational speed in single-phase flow is satisfied in the range of rotational speed 900~1600 min^{-1}. In the case of conventional type of SIso6 w/o OS impeller in air-water two-phase flow, however, it is shown that the gradient of degradation curves of head coefficient ψ becomes gentle with increasing of the rotational speed. In the range of air-water flow rate ratio ϕ_G/ϕ_L>0.10, the head coefficient ψ becomes zero. At the same time, it is confirmed that the shaft power coefficient τ of SIso6 w/o OS impeller approaches asymptotically to zero. On the other hand, in the case of D190_B13 w/o OS developed for air-water two-phase flow operation, the similarity law of the rotational speed is satisfied in water single-phase flow. In air-water two-phase flow condition, it is confirmed that the head coefficient ψ is decreased with the increase of ϕ_G/ϕ_L. However, focusing on the shaft power coefficient τ, the value of τ is not decreased with the increase of ϕ_G/ϕ_L at ϕ_L=0.08 constant. These results have the same tendency in the other water flow coefficient ϕ_L. It is indicated that the difference of degradation curves with changing the rotational speed between SIo6 w/o OS as the conventional type and D190_B13 w/o OS impeller is caused by the difference of the elongation of air-accumulating region in the impeller. From the observation of the air region in the impeller, in the case of SIso6 w/o OS impeller, the air-accumulating region is elongated on the blade pressure surface side[3]. On the other hand, in the case of D190_B13 w/o OS impeller, the air-accumulating region is elongated on the blade suction surface side. We will investigate the difference of occurrence of air-accumulating region in detail as a future works.

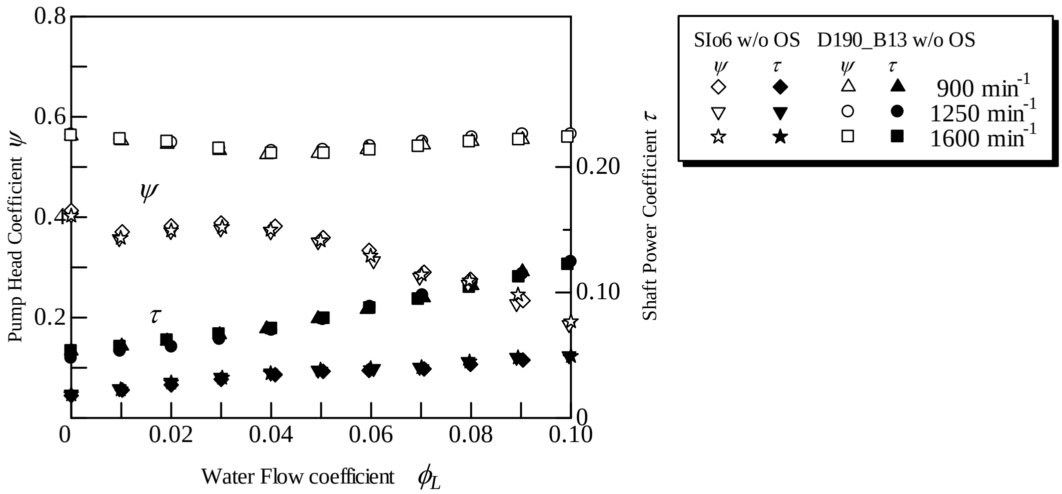

Fig. 3 Pump characteristic curves in single-phase flow with changing of pump rotational speed

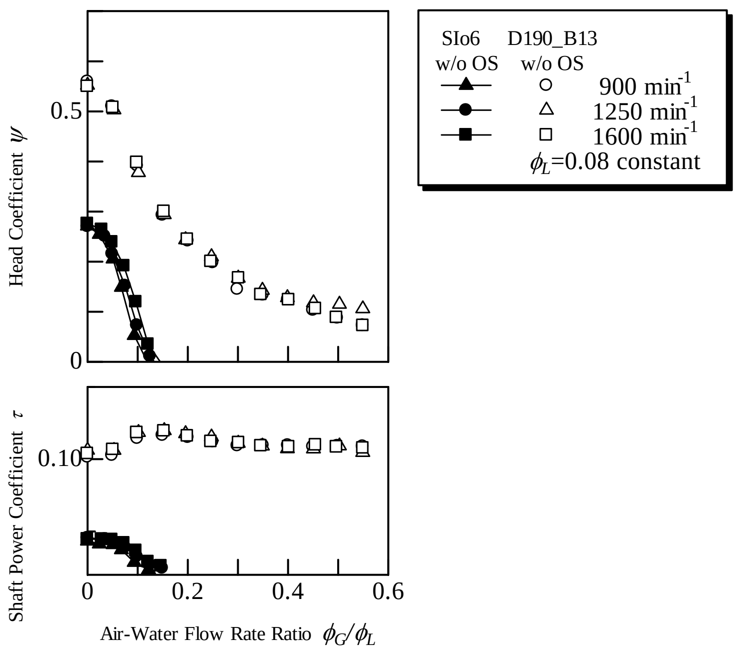

Fig. 4 Pump performances in two-phase flow with changing of pump rotational speed

3.2 Similarity law of impeller configuration

The similarity law of impeller diameter and blade height was investigated experimentally by using the test impellers developed for air-water two-phase flow operation. The similarity law of impeller diameter is clarified by comparing the results between D190_B13 w/o OS, having smaller outlet diameter of D_2=190mm with vaneless diffuser downstream of the impeller outlet, as shown in Fig. 2(a) and D235_B13, having larger outlet diameter of D_2=235mm with no stationary cascade, as shown in Fig. 2(b). Both impellers have blade height of B=13mm and consist of tandem arrangement with double rotating cascade (IR and OR) having forward outlet blade angle β_{2OR}=150^o in OR and β_{2IR}=90^o in IR. The blades of both impellers possess almost the similar geometry in a vertical plane to the pump shaft and the volute casing geometric configuration is the same for all tests. The blade number of D190_B13 w/o OS is Z_{IR}=Z_{OR}=18 and the blade number of D235_B13 is Z_{IR}=Z_{OR}=20. Then the blade numbers was adjusted with taking into account the same blockage ratio of flow passage and peripheral blade thickness effect at the impeller outlet. The peripheral angle of relative position between the inner and outer rotating cascades (IR and OR) is selected[5] as +8º as shown in Fig. 2 to obtain higher two phase flow performance. The test impeller of D190_B13 w/o OS as diffuser pump type and D235_B13 as volute pump type are tested under the case of same volute casing as already stated.

On the other hand, we investigated the similarity law of blade height by using D190_B13 w/o OS impeller having B=13mm and D190_B20 w/o OS impeller having B=20mm. Both impellers have the same diameter of D_2=190mm at the impeller outlet. And then, the diffuser cascade (OS, as shown in Fig. 2(c)) was installed downstream of each impeller outlet in the section of vaneless diffuser. Figure 5 shows the characteristic curve in water single-phase flow, and Fig. 6 shows the degradation curves of air-water two-phase flow performances by changing the air-water flow rate ratio ϕ_G/ϕ_L at ϕ_L=0.08 constant. It should be noted that performances change with air-water flow rate ratio of ϕ_G/ϕ_L at the other flow coefficients of water in almost the same qualitative tendency to results at ϕ_L=0.08 in Fig. 6, though the value itself is different from each other at water flow coefficient and flow rate ratio of air to water.

(1) Influences of impeller diameter

Focusing on the head coefficient curves ψ in water single-phase flow as shown in Fig. 5, the value of D190 impeller (open symbol of circles) is lower than that of D235 impeller (open symbol of upward triangles) in all range of ϕ_L. On the other hand, the shaft power coefficients τ of both impellers (open symbol of circles and upward triangles) take almost the same values at the same ϕ_L. As the results, it might be considered that the similarity law of impeller performances is satisfied and the difference of head coefficient ψ is caused by the differences of passages structure downstream of each impeller. Next, focusing on the air-water two-

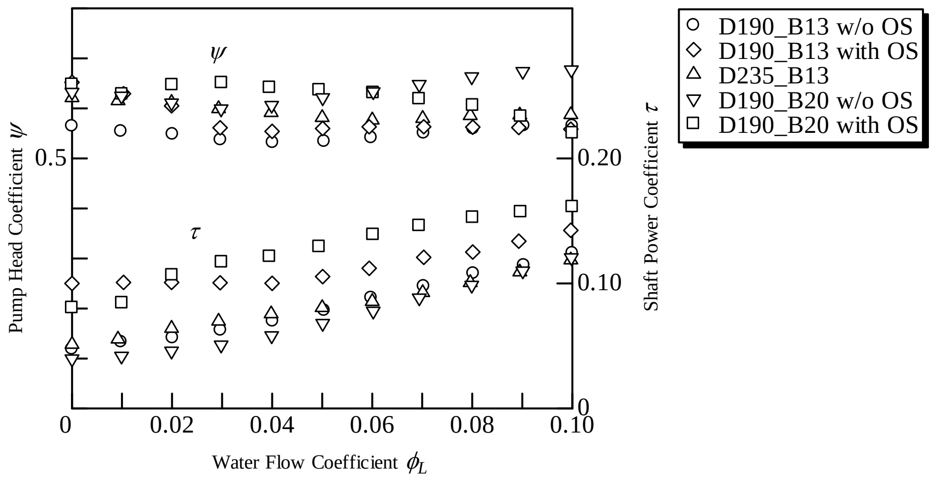

Fig. 5 Pump characteristic curves in single-phase flow

phase flow performances as shown in Fig. 6, the shaft power coefficients τ of both impellers are increased rapidly at ϕ_G/ϕ_L=0.10 due to the use of forward blade. At this operating condition, the jet flows of water from IR cascade to OR cascade and the air-accumulating region at OR cascade appear in both impellers. And the head coefficient ψ of D235 (open symbol of upward triangles) impeller is higher than that of D190 impeller (open symbol of circles). It is considered that this difference is caused by the matching problem of the volute passage as well as the water single-phase flow performances. Figure 7 shows a static head rise coefficient $\Delta\psi_S$ at the pump shroud-wall at ϕ_L=0.08 constant with changing the air-water flow rate ratio ϕ_G/ϕ_L. And we observed air behaviors in the impellers at ϕ_L=0.08 and ϕ_G/ϕ_L=0.16 as shown in Fig. 8. On the static head rise coefficient curves $\Delta\psi_S$ as shown in Fig. 7, we discussed the differences of $\Delta\psi_S$ at three radial positions, IR_{out}=OR_{in} (middle position in radial direction between IR and OR, open and solid symbols of circles), OR_{out} (the outlet of OR cascade, however, the measuring position of OR_{out} has a sudden enlargement from impeller outlet to volute inlet in the case of D235 impeller, open and solid symbols of triangles). The static head rise coefficients $\Delta\psi_S$ of both impellers take almost the same values except the measuring position of OR_{out} of D235 (symbol of solid triangles) downstream of the sudden enlargement from impeller outlet to volute inlet. This result indicates that the similarity law of air-water two-phase flow performances is satisfied as the shaft power coefficient curves in Fig. 6. At the radial measuring position of Volute, there is a significant difference in the value of $\Delta\psi_S$ between both impellers. By

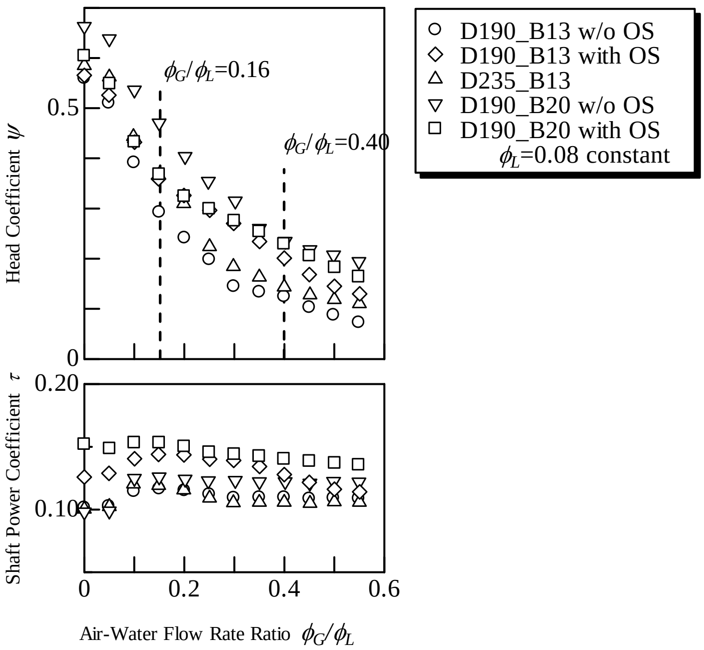

Fig. 6 Air-water two-phase flow performance at ϕ_L=0.08 constant

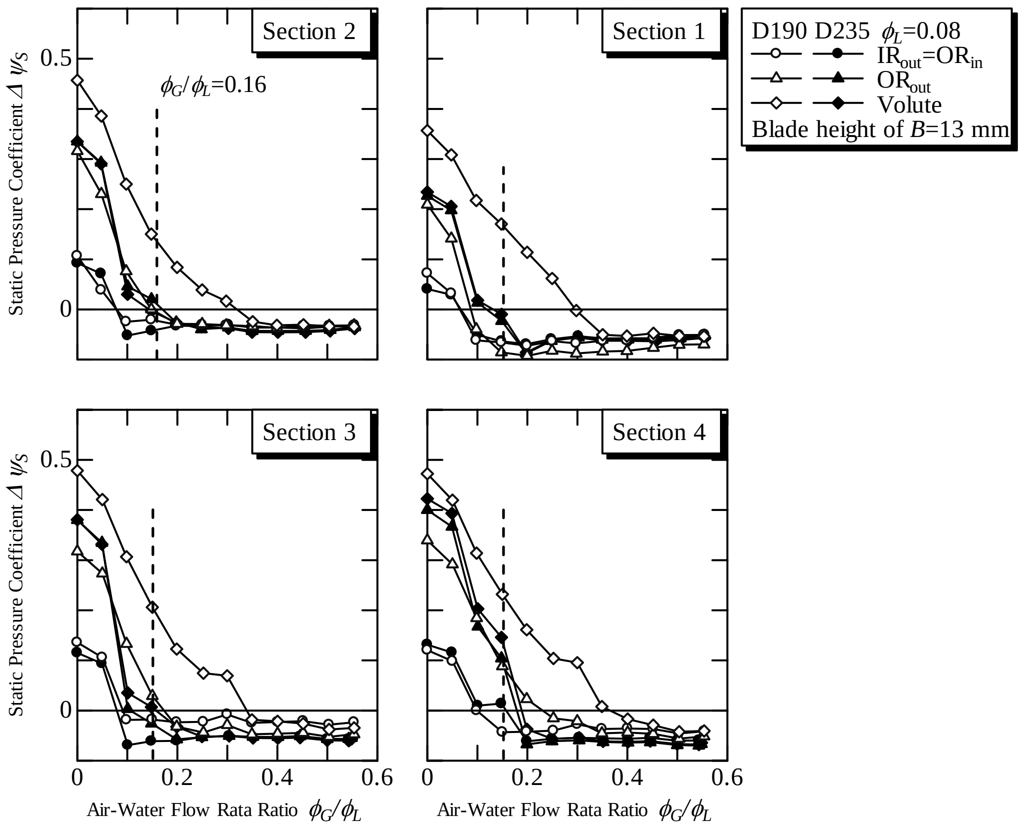

Fig. 7 The static head coefficient curves in air-water two-phase flow at ϕ_L=0.08 constant

comparing the static head rise coefficient between D190 impeller (open symbol of triangles, diffuser pump type) and D235 impeller (open symbol of squares, volute pump type), it might be considered that the installation of vaneless diffuser downstream of impeller outlet contributes to static head recovery in the case of D190 impeller (open symbol of triangles, diffuser pump type). However, pump head coefficient ψ of D235 impeller in Fig. 6 is higher than that of D190 impeller. It is indicated that the dynamic head of D235 impeller recovers to static head rapidly from the Section 4 of volute to delivery pipe.

Figure 9 shows the distributions of measured static head rise coefficient $\Delta\psi_S$ from the radial measuring position of Volute in Section 4 to the delivery pipe. It is confirmed that the static head rise coefficient $\Delta\psi_S$ is recovered rapidly from volute outlet to the delivery pipe. From the observation of the air behaviors in the impellers as shown in Fig. 8, the air accumulating, as a black colored region in the impeller in the figure, is elongated. It is observed that the water jet flows out only from the outer edge of

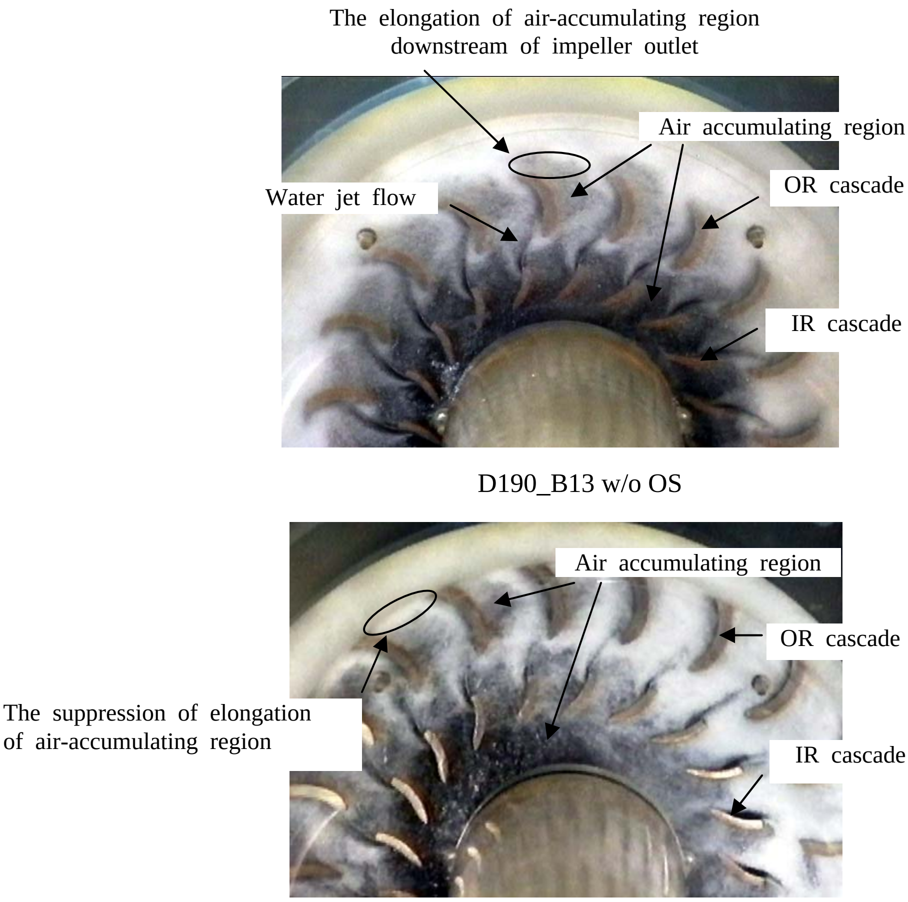

D235_B13

Fig. 8 Air behavior in the impeller at ϕ_L=0.08, ϕ_L/ϕ_G=0.16

pressure surface of IR blades to the pressure surface of OR blades as can be seen as clouded strings in the figure. The jet flow impinges on the blade pressure surface of OR cascade with forward blade and the OR outlet jet flow is turned in the rotating direction. In the case of D190 impeller as a diffuser pump type, it is confirmed that the air-accumulating region on the blade suction surface of OR cascade is elongated downstream of impeller outlet. However, in the case of D235 impeller as a volute pump type, the air-accumulating region on the blade suction surface of OR cascade is sheared and suppressed by higher circumferential flow velocity at volute passage. As a result, it is not observed the air-accumulating region elongated downstream of impeller outlet in the case of D235 impeller. The configuration of test volute is preferable for D235 impeller with larger diameter by considering the results of the static head recovery from the volute to the delivery pipe and the pump head coefficient in air-water two-phase flow condition.

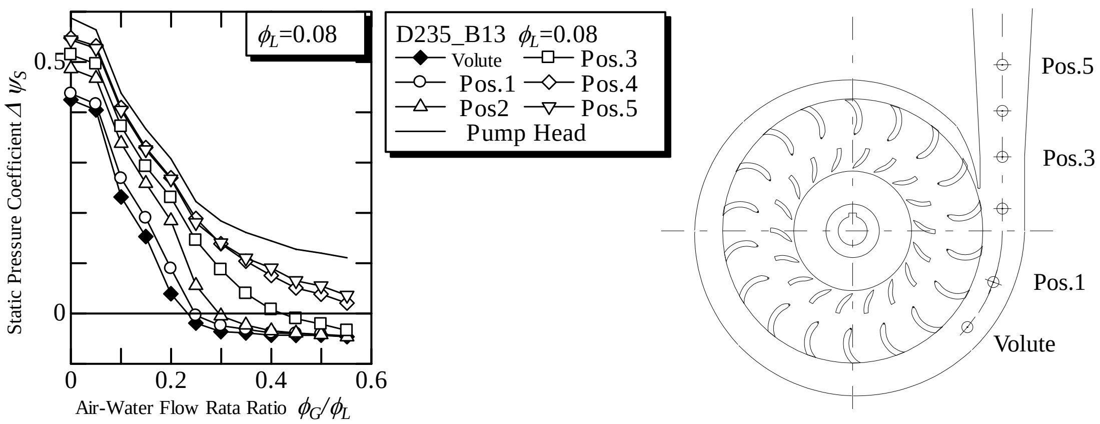

Fig. 9 Static pressure recovery at the delivery pipe in two-phase flow in the case of D235_B13 impeller

(2) Influences of blade height

By comparing the characteristic curves between B20 w/o OS (open symbol of downward triangles) impeller and B13 w/o OS (open symbol of circles) impeller in water single-phase flow as shown in Fig. 5, the pump head coefficient ψ of B20 w/o OS impeller is higher than that of B13 w/o OS impeller in all range of ϕ_L. On the other hand, the shaft power coefficient τ of B20 w/o OS (open symbol of downward triangles) impeller is lower than that of B13 w/o OS (open symbol of circles) impeller. It is considered that the boundary layer in proportion to the main flow is decreased relatively by increasing the main flow region and the three-dimensional flow caused by the curved passage from the suction pipe to impeller inlet has much effect on the impeller outlet flow. On the other hand, under the case of the installation of diffuser cascade (OS) downstream of impeller outlet, the head coefficient ψ of B20 with OS impeller (open symbol of squares), having higher blade height, is higher than that of B13 with OS impeller (open symbol of lozenges) as the results of w/o OS impeller. However, contrary to the results of w/o OS impeller, the shaft power coefficient τ of B20 with OS impeller (open symbol of squares) is higher. It is considered that the installation of diffuser cascade downstream of impeller outlet, particularly in the case of B20 impeller, has much effect on the impeller outlet flow as shown in Fig. 5 (symbol of downward triangles and lozenges). We will clarify this problem due to the measurement of flow distributions in the impeller by using a laser-Doppler velocimetry (LDV) as the future works. In addition to this, the increase of head coefficient ψ of B20 impeller might be caused by the following three factors. Firstly, the degree of sudden enlargement from impeller outlet to the volute inlet is different, that is, the passage height is changed from 13mm or 20mm in the diffuser section to 40mm in volute section. Therefore, the head loss is also changed between both cases. Secondly, the head loss of leakage flow at the blade tip clearance becomes smaller due to the decrease of tip clearance relatively by using higher blade. And finally, the mixing loss of B20 impeller, which is caused by the swirling flow from the impeller outlet and the peripheral flow in the volute passage, is smaller than that of B13 impeller.

The influences of blade height in air-water two-phase flow will be discussed in details by comparing the results of pump characteristic curves at ϕ_L=0.08 constant with changing of ϕ_G/ϕ_L as shown in Fig. 6 and static head coefficient $\Delta\psi_s$ on the shroud wall as shown in Fig. 10. Focusing on the head coefficient curves of ψ, the value of B20 impeller (open symbol of downward triangles and squares in Fig6) is higher than that of B13 impeller (open symbol of circles and lozenges) as a water single-phase flow performances. On the other hand, the shaft power coefficient τ of B20 impeller is lower than that of B13 impeller in the range of ϕ_G/ϕ_L<0.10 as a water single-phase flow performances. However, the shaft power coefficient τ of both impellers are increased rapidly nearly ϕ_G/ϕ_L=0.10, the value of τ of B20 impeller becomes higher by increasing ϕ_G/ϕ_L. In the case of water single-phase flow condition, it is considered that the difference of head coefficient ψ due to the blade height is caused by the head loss of sudden enlargement and mixing loss at the downstream of impeller outlet. In addition to this, in the case of air-water two-phase flow conditions, the change of shaft power coefficient τ is caused by the deflection of air-accumulating region and water jet flow from trailing edge of IR to OR cascade in the blade height direction. These flow deflections have much effect on three dimensional inlet flow due to the increase of blade height in the range of ϕ_G/ϕ_L>0.10. It is noted that the effect of suppression of air-accumulating region due to the leakage flow at the tip clearance is little in the range of higher air-water flow rate ratio[4]. As a

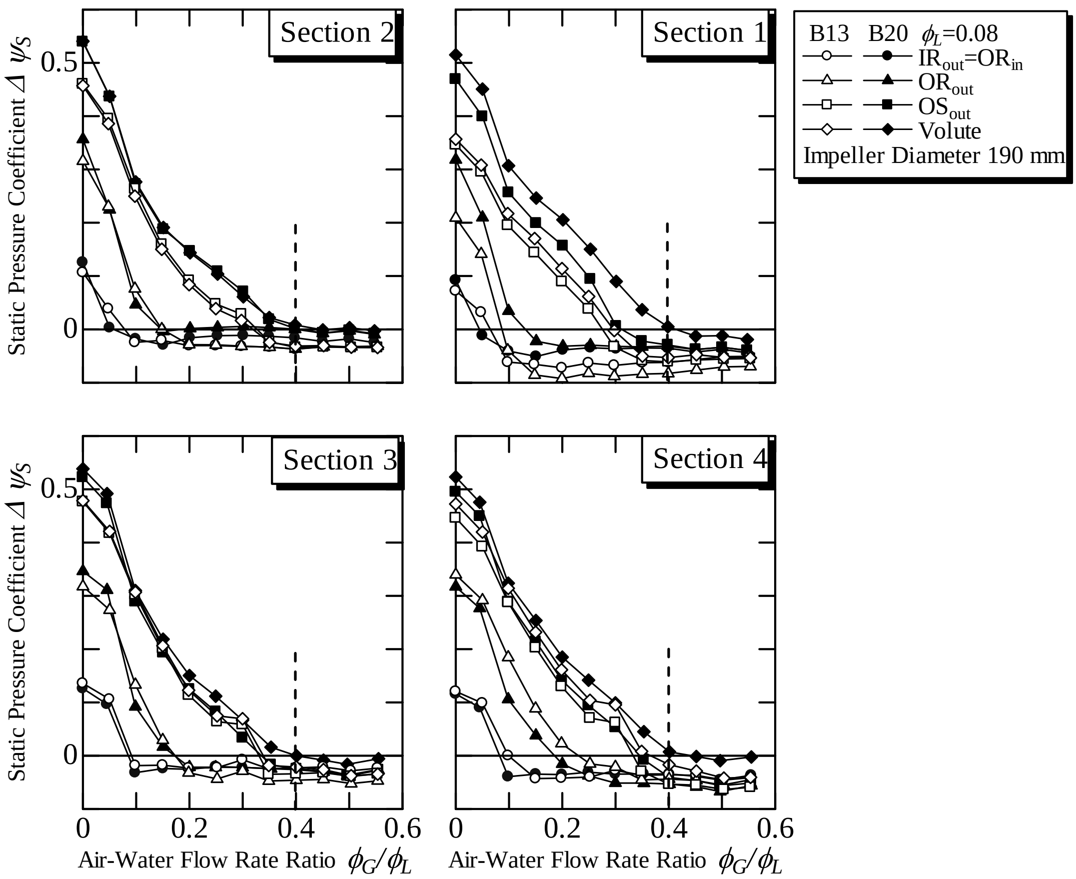

Fig. 10 The static head curve of D190_B13 w/o OS and D190_B20 w/o OS impeller in air-water two-phase flow at ϕ_L=0.08 constant

result, it makes no sense that the difference of pump head coefficient in all range of ϕ_G/ϕ_L as shown in Fig. 6 is caused by the leakage flow at the tip clearance. Figure 10 shows a static head rise coefficient $\Delta\psi_S$. The static head rise coefficients of $\Delta\psi_S$ at outlet of IR cascade (IR_{out}, open and solid symbol of circles) and outlet of OR cascade (OR_{out}, symbol of open triangles and solid triangles) take almost the same value at the most of measuring Sections except Section1 and 4 for both impellers. However, at the measuring position of IR_{out} and Volute, which is downstream of sudden enlargement passage as shown in Fig. 1, the value of $\Delta\psi_S$ of B20 impeller is higher due to the small loss of sudden enlargement and mixing loss. Figure 11 shows air behaviors in the impellers at ϕ_L=0.08 constant and ϕ_G/ϕ_L=0.40. By comparing the air behaviors between ϕ_G/ϕ_L=0.16 as shown in Fig. 8 and ϕ_G/ϕ_L=0.40 as shown in Fig. 11, the air-accumulating region in the IR cascade and on blade suction surface of OR cascade is elongated downstream of OR outlet in the case of w/o OS impeller. It is observed that the water jet flows out only from the outer edge of pressure surface of IR blades to the blade pressure surface of OR cascade as can be seen as clouded strings in these photos. The thickness of water jet of B20 impeller is thicker than that of B13 impeller. And then the static head rise coefficients $\Delta\psi_S$ of both impellers take almost zero as shown in Fig. 10. However, focusing on the head coefficient curves in Fig. 6, the value of head coefficient ψ has positive value of ψ>0. It is indicated that the water jet at the blade pressure surface of OR cascade flows out with the high dynamic head. It might be considered that the difference of air-water two-phase flow performances was caused by the deflection of air-accumulating region and jet flow in the blade height direction due to the difference of blade height. We will investigate the flow distributions by using LDV measurement in detail as a future works. On the other hand, in the case of with OS impeller, the air-accumulating region at the blade suction surface of B13 impeller is observed. But the air-accumulating region of B20 impeller is suppressed even at ϕ_G/ϕ_L=0.40. It is considered that the difference of air-water two-phase flow performances of B13 impeller and B20 impeller is caused by the difference of elongation of air-accumulating region in each impeller.

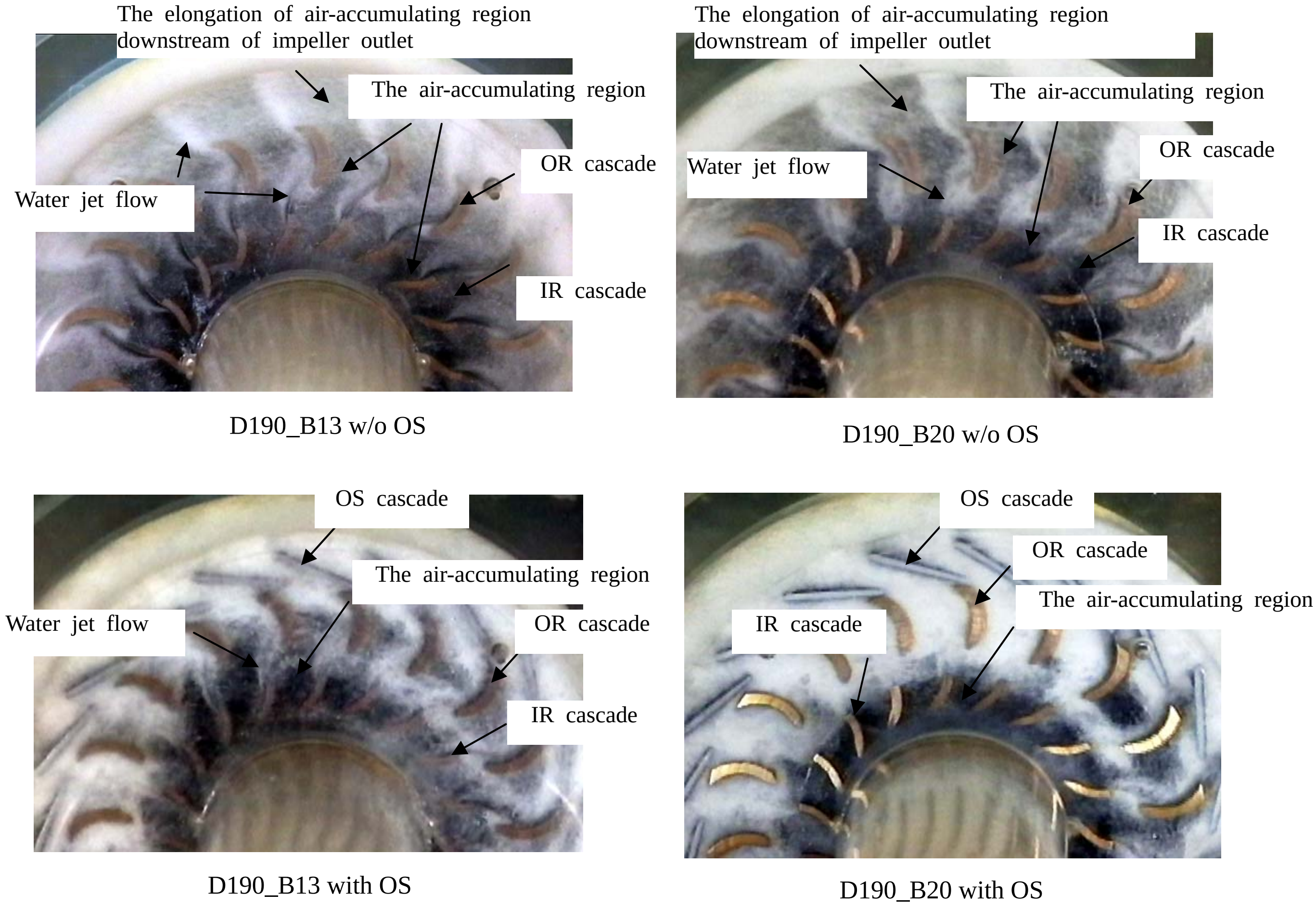

Fig. 11 Air behaviors in the impeller at ϕ_L=0.08, ϕ_L/ϕ_G=0.40

4. Conclusions

The similarity law of impeller diameter, blade height and rotational speed against air-water two-phase flow performance of a centrifugal pump was experimentally investigated. Results are summarized as follows.

(1) The similarity law of rotational speed for the developed impeller with vaneless diffuser is confirmed even in water single-phase flow and air-water two-phase flow.

(2) The dimensionless pump performances of larger impeller with no diffuser and smaller impeller with vaneless diffuser agree well even in two-phase flow under the case of same volute casing.

(3) The dimensionless pump performance of higher blade is superior to that of lower blade under the case of same volute casing. We will investigate the cause of unsatisfactory of similarity law of blade height as a future works.

References

[1] Egashira, K., Furukawa, A. et al., 1996, “Backflow in Twin-Screw-Type Multiphase Pump,” Proc. SPE Annual Tech. Conf., Vol. II, pp. 221-230.

[2] Minemura, K. et al., 1998, “Effects of Design Parameters on Air-Water Two-phase Flow Performance of a Radial-Flow Pump,” Applied Mech. & Eng., Vol. 3-1, pp. 89-109.

[3] Furukawa, A. et al., 1999, “Pumping Action of Centrifugal Impeller with Tandem Circular Cascades in Air-Water Two-phase Flown,” Proc. 3rd ASME/JSME Fluids Eng. Conf., FEDSM99-6773, pp. 1-6.

[4] Furukawa, A. et al., 2003, “Development of Air/water Two-Phase Flow Centrifugal Pump and Its Operating Characteristics,” Proc, 4th ASME/JSME Fluids Eng. Conf., FEDSM03-45013, pp. 1-6.

[5] Furukawa, A. et al., 1990, “Studies on Estimating the Performance of Impellers with Cut-Down of the Blade Edge of the Centrifugal Pump by Surface Singularity Method,” JSME Int. J., Ser.II, 33-3, pp. 525-530.

[6] Furukawa, A. et al., 1996, “Experiments on Air-Water Two-Phase Flow Pump Impeller with Rotating-Stationary Cascades and Recirculating Flow Holes,” JSME Int. J., Ser.B, 39-3, pp. 575-582.

[7] Matsushita, N., Furukawa, A. et al., 2005, “Influences of Impeller Diameter and Diffuser Blades on Air-Water Two-phase flow Performance of centrifugal pump,” Proc. FEDSM2005 ASME Fluids Engineering Division Summer Meeting and Exhibition. FEDSM2005-77388, pp. 1-6.